Trans. Tianjin Univ. 2011, 17: 020-027
DOI 10.1007/s12209-011-1487-6

Dynamic Stability Analysis of Cages in High-Speed Oil-Lubricated Angular Contact Ball Bearings*

LIU Xiuhai(刘秀海)[1], DENG Sier(邓四二)[2], TENG Hongfei(滕弘飞)[1]
(1. School of Mechanical Engineering, Dalian University of Technology, Dalian 116024, China;
2. School of Mechatronics Engineering, Henan University of Science and Technology, Luoyang 471003, China)

Abstract: To investigate the cage stability of high-speed oil-lubricated angular contact ball bearings, a dynamic model of cages is developed on the basis of Gupta's and Meeks' work. The model can simulate the cage motion under oil lubrication with all six degrees of freedom. Particularly, the model introduces oil-film damping and hysteresis damping, and deals with the collision contact as imperfect elastic contact. In addition, the effects of inner ring rotational speed, the ratio of pocket clearance to guiding clearance and applied load on the cage stability are investigated by simulating the cage motion with the model. The results can provide a theoretical basis for the design of ball bearing parameters.

Keywords: dynamic analysis; high-speed angular contact ball bearing; cage; stability; simulation

In high-speed applications such as jet-engines and gyros, the instability of rolling bearing elements might lead to the sudden and catastrophic failure long before the anticipated fatigue life. This leads to the computational modeling and simulation of bearing dynamics to predict the conditions under which such instable motion might occur. Cage stability is one of the most important factors affecting the performance and life of rolling bearings. Thus the investigation of cage instability has received broad attention.

Ball rolling bearings are the primary choice of high speed. Many researchers have developed some dynamic models, and investigated the influencing factors on cage stability. Walter[1] initially developed an analytical model for ball bearing. Gupta[2,3] developed a bearing simulation model ADORE, which is capable of simulating the motion of each bearing element in all six degrees of freedom. By simulating, Gupta investigated the correlation between cage instability and frictional characteristics of lubricant besides the effects of cage clearance, dynamic load and cage unbalance on the cage instability of a solid-lubricated ball bearing. Meeks *et al*[4,5] proposed a dynamic model for the ball bearing in which there are six degrees of freedom for a cage. Kannel, Boesiger, Kingsbury Tateishi and other researchers made a great deal of studies on the dynamics of the cage of ball bearings. In additional, several researchers studied the dynamic characteristics of the cage of cylindrical or tapered roller rolling bearings[6,7].

The cage and balls with six degrees of freedom are considered in Gupta's dynamic model, but oil-film damping and hysteresis damping are not considered, and the contact is assumed as the perfect elastic contact. Although the contact is considered as the non-perfect contact in Meeks' model, but the motion of ball is constrained. Moreover, Meeks' model applies to the solid-lubricated ball bearing.

In China, the studies of the simulation of rolling bearings are mostly focused on cylindrical roller rolling bearings[8-12], and some marked achievements have been made. By contrast, the studies of angular contact ball bearings are fewer, and the quasi-dynamic model rather than three-dimensional dynamic model is used to analyze the angular contact ball bearings[13,14]. The plane model is mainly adopted to analyze the dynamics of the cages in ball bearings[15], while the study of three-dimensional dynamic model of the cage is few.

The objective of this paper is to develop a dynamic model of the cage which is applied to oil-lubricated angular contact ball bearings. The model can simulate the mo-

Accepted date: 2010-08-27.
*Supported by National Key Technology Research and Development Program of China during the 11th Five-Year Plan Period (No. JPPT-115-189) and National Natural Science Foundation of China (No. 50975033).
LIU Xiuhai, born in 1981, male, doctorate student.
Correspondence to TENG Hongfei, E-mail: Tenghf@dlut.edu.cn.

tion of the cage with six degrees of freedom. Particularly, the model introduces oil-film damping between balls and race as well as hysteresis damping acting in a collision, while it does not introduce the motion constraint of balls. With the model, the cage stability in an oil-lubricated angular contact ball bearing will be investigated as functions of inner ring rotational speed, the ratio of pocket clearance to guiding clearance and applied load.

1 Dynamic analytical model

An angular contact ball bearing under oil lubrication is investigated in this paper. The cage of the bearing is guided by the outer ring which is fixed in space. It is assumed that the inner ring rotates at a constant speed. Furthermore, the geometries of the bearing elements are assumed to be perfect, the pockets of cage are cylindrical, and all the mass and geometric centers are assumed to be coincident.

To establish the dynamic equations of the elements, it is required to describe the geometric and kinetic characteristics of the elements. Then the interactions between the elements are computed.

1.1 System description

Various coordinate frames, including an inertial frame, a cage-fixed coordinate frame, ball-azimuth frame and local frame, are defined to describe the geometric and kinetic characteristics of the elements and determine the interactions between the elements. A vector transformation from a frame to another frame can be accomplished by a transformation matrix which is correlative with the Cardan angles between two frames[1,3].

1.2 Analysis of forces

The interactions between the bearing elements have to be investigated for the dynamic model of the cage. Aiming at a high-speed oil-lubricated angle contact ball bearing, we developed a dynamic model in which oil-film damping and hysteresis damping were considered. So the analysis of several forces in this paper is different from that in Refs.[2—5].

1.2.1 Interactions between the ball and race

The interactions between the ball and race consist of the normal force, rolling resistance and tangential friction force.

The hysteresis damping and oil damping between the ball and race are considered, and thus the normal force F_{brN} is calculated by

$$F_{\mathrm{brN}} = K_{\mathrm{P}}\delta^{3/2} + (C_{\mathrm{h}} + C_{\mathrm{o}})u_{\mathrm{rN}} \tag{1}$$

The deformation δ between the ball and race can be determined by using Gupta's method[3]. The Hertzian stiffness K_{P} is calculated in Ref.[16].

Considering the effect of hysteresis, hysteresis damping C_{h} can be obtained by[17,18]

$$C_{\mathrm{h}} = \frac{3K_{\mathrm{P}}\alpha_{\mathrm{e}}\delta^{3/2}}{2}$$

where α_{e} is between 0.08 and 0.32 s/m for steel or bronze.

Oil damping C_{o} is calculated by[19]

$$C_{\mathrm{o}} = c_1 E' R_x^2 G^{c_2} W^{c_3} U'^{c_4} (c_5 - k^{c_6} \mathrm{e}^{k^{c_7}}) \Lambda^{c_8} \mathrm{e}^{-\Lambda^{c_9}} \gamma^{c_{10}}$$

where c_1—c_{10} are constants described in Ref.[19].

The hydrodynamic rolling resistance F_{R} resulting from inlet oil film is calculated by[20]

$$F_{\mathrm{R}} = 2.86 E' R_x^2 k^{0.348} G^{0.022} U^{0.66} W^{0.47} \tag{2}$$

where F_{R} conforms to the reverse direction of u.

The friction force can be calculated by integrating the product of normal stress and traction coefficient over the contact region. To simplify the calculation, the contact region is divided into several elementary strips which are parallel to the minor axis of contact ellipse. The friction force $\mu_i F_{\mathrm{brN}i}$ acting on each strip is calculated. After summing up the forces, the total friction force F_{brT} at the contact can be obtained.

$$F_{\mathrm{brT}} = \sum_i \mu_i F_{\mathrm{brN}i} \tag{3}$$

The friction or traction coefficient is determined by lubrication regime which is evaluated by the oil film parameter $\Lambda = h_{\mathrm{c}} / \sqrt{\sigma_a^2 + \sigma_b^2}$. The calculation of the central film thickness h_{c} is referred to Refs.[21—23].

The oil-lubricated bearing is investigated in this paper, so the traction of the oil film is considered. Under the elastohydrodynamic lubrication (EHL), the friction coefficient μ_{hd} is time-varying as a function of the slide-roll ration and other factors. It is calculated by the empirical formula[24]:

$$\mu_{\mathrm{hd}} = (A + Bs)\mathrm{e}^{-Cs} + D$$

where the coefficients A, B, C and D are the function of normal load, lubricant-inlet temperature, velocity of two contact objects. The detailed procedure is described in Ref.[24].

Under the boundary lubrication, the friction coefficient μ_{bd} is[7]

$$\mu_{\mathrm{bd}} = (-0.1 + 22.28s)\mathrm{e}^{-181.46} + 0.1$$

1.2.2 Interactions between the cage and ball

The cage is assumed to be a rigid rotor. When there is interference between the cage and ball, the interaction

between them is assumed to be a Hertzian contact. Otherwise the interaction is assumed to be purely hydrodynamic without interference[3]. The interaction can be determined by the relative position between the ball and cage as shown in Fig.1.

With the interference between the cage and ball, the normal force F_{bcN} is calculated according to the dry contact by

$$F_{\mathrm{bcN}} = K_{\mathrm{P}}\delta^{3/2} + C_{\mathrm{h}}u_{\mathrm{rN}} \tag{4}$$

With no interference between the cage and ball, the normal force is calculated according to Brewe's isoviscous-rigid lubrication model of a point contact:

$$F_{\mathrm{bcN}} = \frac{U[0.131\arctan(\alpha_{\mathrm{r}}/2)+1.683]}{1+2/(3\alpha_{\mathrm{r}})}\sqrt{\frac{128\alpha_{\mathrm{r}}R_x}{h_{\mathrm{c}}}} \tag{5}$$

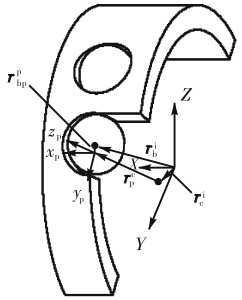

Fig.1 Relative position of a ball and cage

Because the slide between the cage and ball is large, the friction coefficient between the ball and cage is assumed to be a constant μ_{bc}. Thus the tangential friction force is

$$F_{\mathrm{bcT}} = \mu_{\mathrm{bc}}F_{\mathrm{bcN}} \tag{6}$$

1.2.3 Interactions between the cage and outer ring

The hypotheses of the cage-ball interactions are used to define the cage-ring interactions shown in Fig.2. It has to be done first to analyze whether there is a contact between the ring and cage. If there is a contact, the force is calculated according to the Hertzian contact, otherwise the force is calculated according to the short journal bearing model[25].

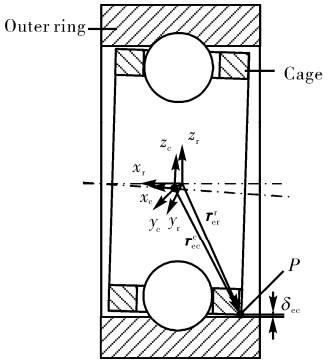

Fig.2 Cage-ring interactions

The azimuth of the point with the minimum clearance or maximum interference in the cage frame is solved by a globally convergent Newton's method. Then the interference between the cage and ring δ_{ec} is obtained.

In the case of $\delta_{\mathrm{ec}} \geqslant \Delta_{\mathrm{r}}$, the interactions between the ring and cage are evaluated by the slice technique in order to handle the incline of the cage. The process includes the following steps: dividing the cage into several thin disks; judging the amount of the disks in contact with the ring; and then computing the interactions between the ring and disks. Consequently these local interactions are integrated to obtain the total ring-cage interaction.

In this case, the normal force between the cage and the *j*th disk is calculated by

$$F_{\mathrm{crN}j} = K_{\mathrm{L}}\delta_j^{10/9} + C_{\mathrm{h}}u_{\mathrm{rN}j} \tag{7}$$

The tangential force between the cage and the *j*th disk is

$$F_{\mathrm{crT}j} = \mu_{\mathrm{cr}}F_{\mathrm{crN}j} \tag{8}$$

where μ_{cr} is a Coulomb friction coefficient.

If $\delta_{\mathrm{ec}} < \Delta_r$, the interactions between the cage and ring can be evaluated according to the short journal bearing model. The forces and moment are obtained by[25]

$$F_{\mathrm{cr1}} = -\frac{\eta u l^3\varepsilon^2}{c^2(1-\varepsilon^2)^2} \tag{9}$$

$$F_{\mathrm{cr2}} = \frac{\pi\eta u l^3\varepsilon}{4c^2(1-\varepsilon^2)^{3/2}} \tag{10}$$

$$M_{\mathrm{crx}} = \frac{2\pi\eta v R_{\mathrm{cr}}^2 L}{c} \tag{11}$$

In the above three-dimensional mechanical model of the cage and ball, the time-varying traction forces of lubricant are considered, meanwhile oil-film damping between the balls and race as well as hysteresis damping acting in a collision are introduced. The model better corresponds with the actual conditions.

1.3 Dynamic differential equations

Based on Newton's law of motion, the translational motion of the cage mass center can be written in the Cartesian coordinates as

$$\begin{cases} m_{\mathrm{c}}\ddot{x}_{\mathrm{c}} = \sum F_{\mathrm{cx}} \\ m_{\mathrm{c}}\ddot{y}_{\mathrm{c}} = \sum F_{\mathrm{cy}} \\ m_{\mathrm{c}}\ddot{z}_{\mathrm{c}} = \sum F_{\mathrm{cz}} \end{cases} \tag{12}$$

The differential equations for the rotational motion of the cage around its mass center can be described by the classical Euler equations of motion as

$$\begin{cases} I_1\dot{\omega}_{\mathrm{c1}} - (I_2 - I_3)\omega_{\mathrm{c2}}\omega_{\mathrm{c3}} = \sum M_{\mathrm{c1}} \\ I_2\dot{\omega}_{\mathrm{c2}} - (I_3 - I_1)\omega_{\mathrm{c1}}\omega_{\mathrm{c3}} = \sum M_{\mathrm{c2}} \\ I_3\dot{\omega}_{\mathrm{c3}} - (I_1 - I_2)\omega_{\mathrm{c1}}\omega_{\mathrm{c2}} = \sum M_{\mathrm{c3}} \end{cases} \tag{13}$$

where M_{c1}, M_{c2} and M_{c3} are the components of various applied moments in the cage-fixed coordinate frame.

The orientation of the cage is tracked by defining the orientation of the cage-fixed frame relative to the inertial frame through Cardan angles. The relationship between Cardan angles and angular velocity and acceleration can be found in Refs.[1] and [3].

In the cylindrical system of the inertial frame, Newton's equations of motion of a single ball mass center is

$$\begin{cases} m_b\ddot{x}_b = \sum F_{bx} \\ m_b\ddot{r} - m_b r\dot{\theta}^2 = \sum F_{br} \\ m_b r\ddot{\theta} + 2m_b\dot{r}\dot{\theta} = \sum F_{b\theta} \end{cases} \tag{14}$$

In the ball-azimuth frame, Euler equations of motion of a single ball is

$$\begin{cases} I_b\dot{\omega}_1 = \sum M_1 \\ I_b\dot{\omega}_2 - I_b\omega_3\dot{\theta} = \sum M_2 \\ I_b\dot{\omega}_3 + I_b\omega_2\dot{\theta} = \sum M_3 \end{cases} \tag{15}$$

In this paper, the inner ring of the bearing rotates at a constant angular velocity, and the overturning moment and variable torque are not considered, so only three differential equations for the translational motion of the inner ring, which are the same as Eq.(12), are taken into account.

1.4 Solving procedure of the dynamic model

The basic steps of solving the dynamic model are shown in Fig.3. The initial conditions for the integration of the differential equations of motion are first determined from the geometric constraints and kinetic conditions by a quasi-static analytical model. Then the local interactions between the bearing elements are identified depending on the relative position and relative motion of the elements, thus the applied forces and moments are obtained by Eqs.(1)—(11). After that, the total forces and moments are determined. Finally, the differential equations are integrated with the fourth-order method which can vary step size automatically. Then the real-time position and velocity variables of the cage are obtained.

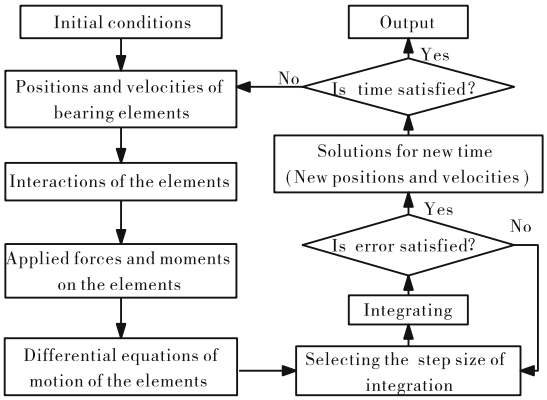

Fig.3 Solving procedure of the dynamic model

1.5 Verification and comparison

A classic ball bearing, the cage mass center orbit of which was measured and simulated by Gupta, was considered to verify the dynamic analytical model developed in this paper. The parameters of the bearing are listed in Tab.1, and more data are described in Ref.[3]. The cage mass center orbits obtained through the experiment and simulation are shown in Fig.4.

Tab.1 Geometries of the bearing for verification

Parameter	Value
Bearing inside diameter/mm	100
Bearing outside diameter/mm	180
Ball diameter/mm	19.05
Number of balls	18
Contact angle/(°)	25°
Cage guide surface	Outer ring
Inner race curvature factor	0.54
Outer race curvature factor	0.52
Cage-ring guiding diametrical clearance/mm	1.460 5
Pocket clearance/mm	0.863 6

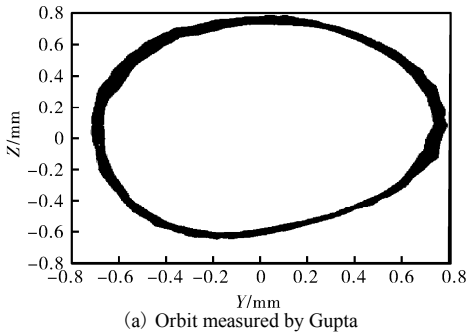

(a) Orbit measured by Gupta

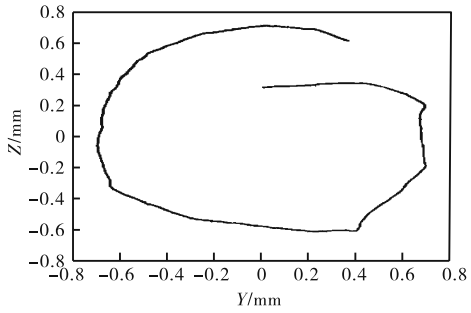

(b) Orbit predicted by Gupta

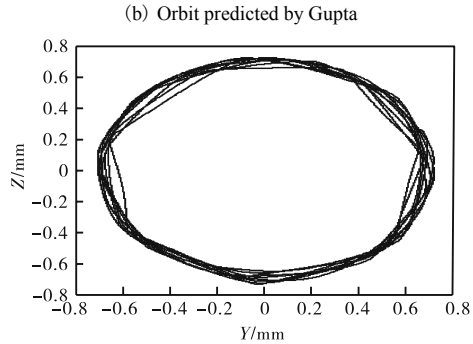

(c) Orbit predicted by the model in this paper

Fig.4 Cage mass center orbit at 10 000 r/min

From Fig.4, it is seen that the orbit simulated by the model developed in this paper is in reasonable agreement with the experimental orbit. The orbit is under steady condition. The small differences in the orbit radii, as Gupta remarked, are probably due to the uncertainty of the clearance between the cage and ring[3]. The orbit simulated by Gupta does not reach a steady state because there are a limited number of circles in the process. It is proved that the capability of the model developed in this paper to predict the motion of cage is desirable, and it is feasible and reliable to analyze the dynamic performance of the cage by the model.

1.6 Instability criterion of the cage

Since instable orbits correspond to erratic motion, the translational speed of the cage mass center can be used as a quantitative criterion for cage stability. For stable operation, the cage mass center orbit is almost circular, and very small variations in speed are observed, while large variations correspond to erratic operation[6]. In the following section, we will discuss the cage stability which is affected by inner ring rotational speed, the ratio of pocket clearance to guiding clearance and applied load. The criterion of the cage instability in Ref.[6] is introduced for the discussion in this paper. The degree of instability of cage is defined as the ratio of the standard deviation of the cage center translational speed to its mean value, i.e., the speed deviation ratio. The smaller value of the ratio corresponds to more stable cage motion.

2 Simulation results

The geometries and mass parameters of the high-speed angle contact ball bearing investigated in this paper are shown in Tab.2. The bearing is lubricated with aviation lubricant. It takes a period of time to reach a steady state from the initial state. Therefore, we investigated the data of simulation from the 25th to the 45th shaft revolution. The effects of various parameters on the cage stability are estimated by analyzing the data.

Tab.2 Bearing geometries and mass parameters

Parameter	Value
Cage outside diameter/mm	34.25
Cage inside diameter/mm	29.15
Cage pocket diameter/mm	6.7
Cage mass/g	15.7
Cage width/mm	11.40
Cage-ring guiding radial clearance/mm	0.25
Bearing bore/mm	20
Bearing outside diameter/mm	42
Pitch diameter/mm	31
Inner race curvature factor	0.53
Outer race curvature factor	0.55
Number of balls	12
Ball diameter/mm	6.35

We normalized the radial and axial positions of the cage with the guiding clearance between the cage and the outer ring in the following section.

2.1 Effect of inner ring rotational speed on cage stability

Fig.5 and Fig.6 show the orbits and speed deviation ratio of the cage mass center at various inner ring rotational speeds when the axial load is 100 N. In these cases, all the cage mass center orbits are almost circular and regular, which means the cage is stable. However, in Fig.6 there is still a small fluctuation in the cage center translational motion, indicating that there are some collisions between the balls and cage or between the race and cage. When the inner ring rotational speed is higher than 30 000 r/min, the speed deviation ratio of the cage decreases, and the stability increases with increasing inner ring rotational speed. When the speed is high, the geometric coupling between the cage and ball is high, and thus the collision reduces and the variation in the speed of the cage mass center is small.

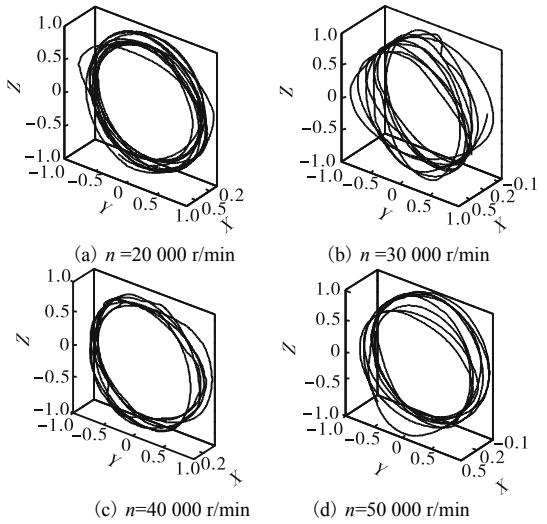

Fig.5 Cage mass center orbits at various inner ring rotational speeds

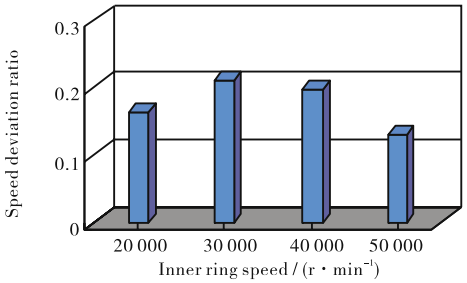

Fig.6 Cage instability at various inner ring rotational speeds

2.2 Effect of cage pocket clearance and guiding clearance on cage stability

The effect of the clearance ratio on cage stability was investigated. The clearance ratio c is defined as a ratio of the cage pocket clearance to the guiding clearance between the cage and the outer ring. The pocket clearance varies while the guiding clearance between the cage and the outer ring remains unchanged at the inner ring rotational speed of 30 000 r/min when the axial load is 100 N.

Fig.7 and Fig.8 show the orbits and speed deviation ratio of the cage mass center for various clearance ratios. The orbits are regular for clearance ratio less than 1. The speed deviation ratio increases with the increase of the clearance ratio. If the clearance ratio is more than 1, the cage mass center orbit becomes irregular, and cage instability rises. Therefore, a large clearance ratio is not suitable for the stable motion of the cage. This is because there are more offset spaces for the balls if the clearance ratio is greater than 1, and the randomness of collisions between the cage and balls increases. Meanwhile, the cage might collide with the outer ring, and a large friction is introduced. Then the cage orbit becomes irregular, and the speed deviation ratio becomes large.

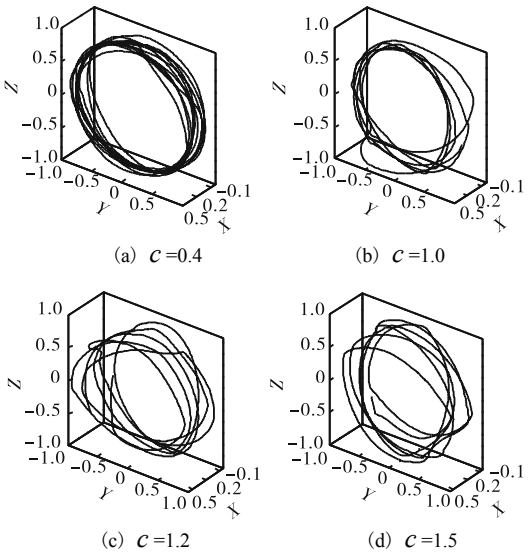

Fig.7 Cage mass center orbits for various clearance ratios

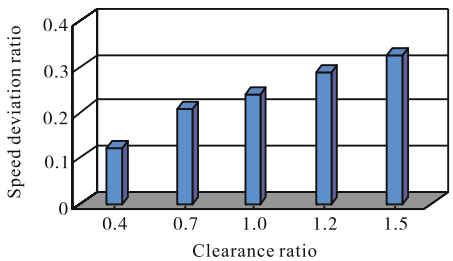

Fig.8 Cage instability for various clearance ratios

2.3 Effect of axial load on cage stability

It is assumed that the bearing operates only under an axial load F_a when the inner ring rotational speed is 30 000 r/min. For the axial loads of 50 N, 100 N, 200 N, 300 N and 500 N, the cage orbits and speed deviation ratios are shown in Fig.9 and Fig.10. It is seen that the cage orbits are regular in all the cases, while cage stability is enhanced with the increase of axial load. The large axial load restricts the slide of balls and makes the ball operate stably, thus the collision between the ball and cage reduces. Therefore, loading an appropriate axial force on an angular contact ball bearing is required to keep the cage motion stable. However, the axial load can not be too large, in that case the excessive friction and wear would take place.

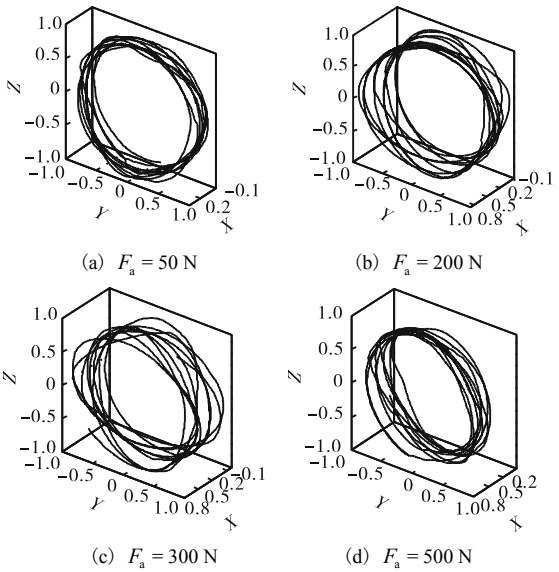

Fig.9 Cage mass center orbits under various axial loads

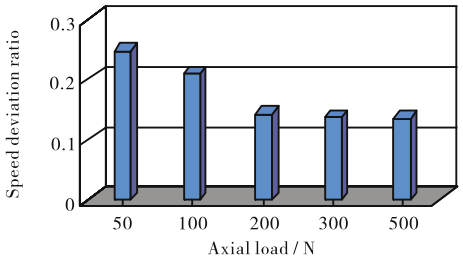

Fig.10 Cage instability under various axial loads

2.4 Effect of damping on cage stability

The coefficient α_e is an important factor to define the magnitude of damping. The larger α_e, the more powerful damping. Fig.11 shows the effect of α_e on cage stability. Cage stability becomes better with the rise of α_e, i.e., large damping is beneficial to cage stability. In addition, the introduction of damping makes it quicker to solve the dynamic equations.

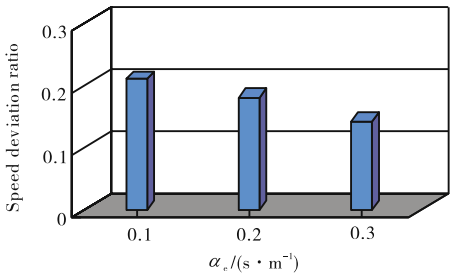

Fig.11 Cage instability at various values of α_e

3 Conclusions

In this paper, aiming at the cage stability of high-speed oil-lubricated angular contact ball bearings, a dynamic analytical model of the cage is developed. In the model, an empirical formula is employed to calculate the traction coefficient of lubricating oil. The model also introduces oil-film damping between the balls and race as well as hysteresis damping acting in the collision.

The cage motion in an oil-lubricated angular contact ball bearing was analyzed for various operating conditions and geometric parameters by the model developed in this paper. The effects of the operating conditions and geometric parameters on cage stability are as follows.

(1) The cage mass center orbit is almost circular at high inner ring rotational speed under an axial load. The cage instability decreases with the increase of the inner ring rotational speed.

(2) The cage instability is enhanced when increasing the pocket clearance. Particularly, when the ratio of the pocket clearance to the guiding clearance is more than 1, the cage instability is enhanced sharply, and the cage mass center orbit becomes irregular. This trend is similar to what Gupta showed for a solid-lubricated bearing. Thus, for the cage in an oil-lubricated bearing, the ratio of the pocket clearance to the guiding clearance also has a close relation to the cage stability.

(3) The large axial load benefits steady motion of the cage, but it also reinforces friction and heating in the bearing. Therefore, it is necessary to apply appropriate axial loads to bearing design.

(4) The larger the damping, the more stable the motion of the cage.

The six-degree-of-freedom dynamic model can be used in parameter optimization design of angular contact ball bearings.

Nomenclatures

c —radial guiding clearance;

C_h —hysteresis damping;

C_o —oil damping;

E' —equivalent elastic modulus;

F —applied force;

F_{cx}, F_{cy}, F_{cz} —components of applied force on the cage;

F_{bx}, F_{br}, $F_{b\theta}$ —components of applied force on the ball in the cylindrical inertial frame;

G —dimensionless material parameter, $G = \alpha E'$;

h_c —central film thickness;

I_1, I_2, I_3 —principal moments of inertia of the cage;

I_b —principal moment of inertia of the ball;

L —width of the guiding land of the cage;

l —width of the line contact;

k —ellipticity ratio;

K_P —Hertzian stiffness of point contact;

K_L —Hertzian stiffness of line contact, $K_L = 0.356E'l^{8/9}$;

M —applied moment;

M_{cx} —shear torque of oil;

m_b —mass of a ball;

m_c —mass of the cage;

R_{cr} —guided radius of the cage;

R_x, R_y —equivalent curvature radii along the minor and major axes of contact ellipse;

s —slide-roll ratio, $s = (u_a - u_b)/u$;

u —mean velocity;

u_a, u_b —surface velocities of two mating ellipsoids a and b;

u_{rN} —normal component of relative velocity;

U —dimensionless velocity parameter, $U = \eta_0 u/(E'R_x)$;

U' — $U' = 2U$;

v —relative velocity;

W —dimensionless load parameter, $W = w/E'R_x^2$;

w —normal load;

x_c, y_c, z_c —position components of the cage;

x_b, r, θ —position components of the ball in the cylindrical inertial — frame;

α —viscosity-pressure coefficient;

α_e —coefficient relevant to the coefficient of restitution;

α_r —radius ratio, $\alpha_r = R_y/R_x$;

γ —surface pattern parameter;

Δ_r —critical clearance;

δ —elastic deformation;

ε —eccentric ratio;

η_0 —dynamic viscosity at atmospheric pressure;

Λ —oil film parameter;

μ —friction coefficient;

μ_{bd} —friction coefficient under boundary lubrication;

μ_{hd} —friction coefficient under EHL;

σ_a, σ_b —surface roughness of bodies a and b;

ϕ_T —thermal correction factor of the oil film;

ω —angular velocity.

References

[1] Walter C T. The dynamics of ball bearings[J]. *Journal of Lubrication Technology*, 1971, 93(1): 1-10.

[2] Gupta P K. Dynamics of rolling element bearings. Parts I, II, III and IV[J]. *Journal of Lubrication Technology*, 1979, 101(3): 293-326.

[3] Gupta P K. *Advanced Dynamics of Rolling Elements*[M]. Springer Verlag, New York, 1984.

[4] Meeks C R, Ng K O. The dynamics of ball separators in ball bearings (Part I): Analysis[J]. *Tribology Transactions*, 1985, 28(3): 277-287.

[5] Meeks C R, Tran L. Ball bearing dynamic analysis using computer methods (Part I): Analysis[J]. *Journal of Tribology*, 1996, 118(1): 52-58.

[6] Ghaisas N, Wassgren C R, Sadeghi F. Cage instabilities in cylindrical roller bearings[J]. *Journal of Tribology*, 2004, 126(4): 681-689.

[7] Sakaguchi T, Harada K. Dynamic analysis of cage behavior in a tapered roller bearing[J]. *Journal of Tribology*, 2006, 128(3): 604-611.

[8] Chen G, Li J, Zhang C. Analysis of the interaction between high speed bearing components[J]. *Mechanical Science and Technology*, 1998, 17(2): 268-270 (in Chinese).

[9] Cui L, Wang L, Zheng D *et al*. Analysis on dynamic characteristics of aero-engine high-speed roller bearings [J]. *Acta Aeronautica ET Astronautica Sinica*, 2008, 29(2): 492-498 (in Chinese).

[10] Li J, Wu L. Dynamic simulation of high-speed roller bearings[J]. *Journal of Aerospace Power*, 1993, 8(2): 112-116 (in Chinese).

[11] Yang X, Liu W, Li X. Dynamics analysis on cage of high speed roller bearing[J]. *Bearing*, 2002(7): 1-5 (in Chinese).

[12] Zhang C, Cheng G, Li J. Dynamic analysis of high speed roller bearings[J]. *Mechanical Science and Technology*, 1997, 16(7): 136-139 (in Chinese).

[13] Luo Z, Wu L, Sun X *et al*. Quasidynamic analysis of high speed thrust ball bearings[J]. *Journal of Aerospace Power*, 1996, 11(3): 257-260 (in Chinese).

[14] Wang L, Cui L, Zheng D *et al*. Analysis on dynamic characteristics of aero-engine high-speed ball bearings[J]. *Acta Aeronautica ET Astronautica Sinica*, 2007, 28(6): 1461-1467 (in Chinese).

[15] Deng S, Hao J, Teng H *et al*. Dynamics analysis on cage of angular contact ball bearings[J]. *Bearing*, 2007(10): 1-5 (in Chinese).

[16] Harris T A. *Rolling Rearing Analysis*[M]. John Wiley, New York, 2001.

[17] Herbert R G, McWhannell D C. Shape and frequency composition of pulses from an impact pair[J]. *Journal of Engineering for Industry*, 1977, 99(3): 513-518.

[18] Hunt K H, Crossley F R E. Coefficient of restitution interpreted as damping in vibroimpact[J]. *Journal of Applied Mechanics*, 1975, 42(2): 440-445.

[19] Sarangi M, Majumdar B C, Sekhar A S. Stiffness and damping characteristics of lubricated ball bearings considering the surface roughness effect (Part 1 and 2)[J]. *Journal of Engineering Tribology*, 2004, 218(6): 529-547.

[20] Houpert L. Numerical and analytical calculations in ball bearings [C]. In: *Proceedings of the 8th European Space Mechanisms and Tribology Symposium*. Toulouse, France, 1999. 283-290.

[21] Chittenden R J, Dowson D, Dunn J F *et al*. A theoretical analysis of the isothermal elastohydrodynamic lubrication of concentrated contacts (II): General case with lubricant entrainment along either principal axis of the Hertzian contact ellipse or at some intermediate angle[J]. *Proceedings of the Royal Society of London, Series A: Mathematical and Physical Sciences*, 1985, 397(1813): 271-294.

[22] Gupta P K, Cheng H S, Zhu D *et al*. Viscoelastic effects in MIL-L-7808-Type lubricant (Part I): Analytical formulation[J]. *Tribology Transactions*, 1992, 35(2): 269 - 274.

[23] Hamrock B J, Schmid S R, Jacobson B O. *Fundamentals of Fluid Film Lubrication*[M]. Marcell Dekker, Inc, New York, 2004.

[24] Wang Y S, Yang B Y, Wang L Q. Investigation into the traction coefficient in elastohydrodynamic lubrication[J]. *TriboTest*, 2004, 11(2): 113-124.

[25] Cameron A. *Basic Lubrication Theory* [M]. Ellis Horwood Ltd, Chichester, 1981.